Desalination and Water Treatment
www.deswater.com

1944-3994/1944-3986 © 2012 Desalination Publications. All rights reserved
doi: 10/5004/dwt.2012.2499

Taylor & Francis
Taylor & Francis Group

42 (2012) 144–154
April

Thermodynamic diagnostic of electrons densities in gas bubbles in aerated saturated refinery wastewater

Mirjana Miladin Ševaljević[a,*], Stojan Nikola Simić[b], Petar Vlado Ševaljević[c]

[a]*High Technical School, Đorđa Stratimirovića 23, in Zrenjanin, University of Novi Sad, Serbia*
Tel./Fax: 381 23 565 896; email: sevaljevic.mirjana @gmail.com
[b]*Oil refinery a.d. Modriča, Bosnia and Herzegovina*
[c]*Petrol, Ljubljana, Slovenija*

Received 20 October 2010; Accepted 29 August 2011

ABSTRACT

Electro-chemical potentials of adsorbed hydrogen on active centers could help energy efficiency of oxygen transport in the aerated saturated refinery wastewater to be optimized. In stationary regime, by using of the same membrane diffuser, the true understanding of the spontaneous fastest parallel exchange of electrons by Boltzmann collisions and slowest oxygen mass diffusion transport by adsorption can be attained. This paper presents diagnostic of electrons density in the gas bubbles in aerated saturated refinery wastewater, according to the criteria of partial local thermodynamic equilibrium (PLTE). By the different stationary air flows, different water tank height and different motor oil content it was obtained that water entropy driven electrons density transport through the monolayer of the adsorbed air bubble controls energy efficiency of oxygen transport.

Keywords: Perforated membrane air distributor; Refinery waste water; Aeration regimes; PLTE of electrons and hydrogen ions; Saturated water; Polarized air bubbles; Electrons densities; Aeration energy efficiency

---

1. Introduction

By the final result of the aeration process described in our prior paper were shown the energy efficiencies of oxygen transport with greater water height 2 m without added motor oil content and with less air flows were greater in comparison with greater air flows. Experimental procedure and obtained results were described in our prior paper [1].

In this paper the influence of water aeration regime on energy efficiency of oxygen transport in water column with water height 1 m as well as 2 m, with the same membranes diffuser was examined.

The obtained results could be explained by Boltzmann electrons distribution, in the two energy states by collisions according to the criteria of partial local thermodynamic equilibrium (PLTE).

2. Experimental

In various biology treatments of technological wastewater and communal waters aeration by perforated membranes distributer fixed with a ring over disc of material (PA GF30) with material EPDM (ethylene-propylene-dimer) "Gummy-Jaeger" can be applied, on water temperatures 5°C to 35°C and on air input has to be less than 60°C [2] (Table 1, Fig. 1). The using age of membrane of distributers is 10 y and depends of

---

*Corresponding author.

Table 1
Caracteristics of membranes distributors

Type	Aerated surface (m^2)	Air flow ($m^3\ h^{-1}$)	Material of disc	Membrane material
HD 270	0.037	1.5–7	PP GF30	EPDM/ silicon
HD 340	0.060	2–10	PP GF30	EPDM
HD 235	0.030	1.5–7	PA GF30	EPDM
HD 325	0.059	2–10	PA GF30	EPDM
ECO 21	0.045	1.5–7	PP GF30	EPDM
ECO 34	0.045	2–10	PP GF30	EPDM

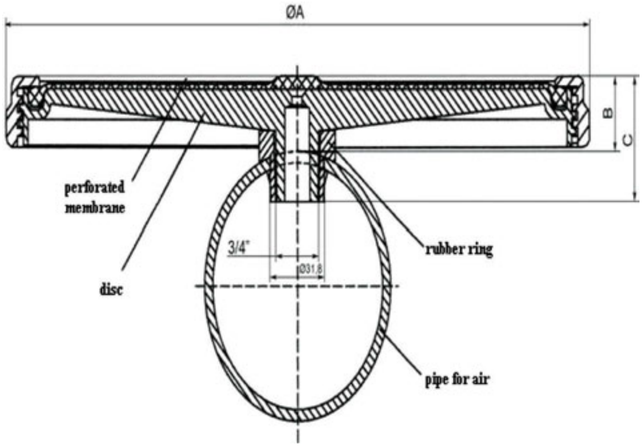

Fig. 1. Disk-shaped membrane air distributor.

wastewater characteristics and parameters of aeration process, but the control has to be made at least once per year. At standard conditions air flow is regulated in dependent of oxygen demand according to recommended for the distributer type [2–5].

The greater air flow increase dimensions of the bubbles and decrease efficiency of oxygen transport. The smaller air flows cause the smaller efficiency of aeration surface of distributer.

In order to determine technical characteristics of an aeration system with different water height 1 and 2 m it was necessary to first determine the volume coefficient of oxygen transport in wastewater, k_La, by method according to [1,6]: capacity, oxygen transport efficiency and energy efficiency of oxygen transport.

A polypropylene column with dimensions 700 × 700 × 2200 mm and accompanying connections and framework was used for experimental work in batch conditions. The cross-section surface of the column was defined according to recommendations for an air distributor.

Experimental work was performed for batch working conditions and varying air flow of 2 and 10 $m^3\ h^{-1}$. The water level in the column was 1 and 2 m high and the total volume was 490 and 980 l. Water aeration with waste oil content of 5 and 10 mg l^{-1} was performed. Dissolved oxygen was previously removed using a chemical method. Investigation of aeration of clean water not containing dissolved oxygen was also performed to be able to compare process parameters for air distribution in standard investigation conditions with the ones obtained in real conditions for wastewater with corresponding characteristics. Average characteristic of wastewater in Refinery in Modriča, in period of investigation were: pH in range 7–8, temperature 15°C–25°C, oil content 13–23 mg l^{-1}, inorganic salts 0.38–0.40 mg l^{-1}, TSS 0.5–0.7 mg l^{-1}, HPK 80–180 mg l^{-1} BPK, up to 0–7 mg l^{-1}, CaO 18.5–21.5 mg l^{-1} and electric conductivity 670–770 µS cm^{-1}. Characteristic of examined water are dependent of content of added motor oil content up to zero as 5 and 10 g m^{-3} of the added viscous waste motor oil (SAE 15 W-40, with 132.0 $mm^2\ s^{-1}$ viscosity index; with inflammation temperatures of 231.0°C; with 3.18 mg KOH g^{-1} TAN; as 9.73 mg KOH g^{-1} TBN; with content of 0.039% Zn; 0.310% Ca; 13.4 ppm Fe; 4.11 ppm Cu; 0.98 ppm Cr and 44.87 ppm Al). Densities of three examined samples of water were in range of 992–996 kg m^{-3}, viscosity in range of 0.81×10^{-6}–$0.99 \times 10^{-6}\ m^2\ s^{-1}$ and surface tension coefficients were 76.2; 64.8 and 57.3 mN m^{-1}, respectively.

A defined amount of waste oil was dosed into the water. A complete investigation regime for defining process parameters of aeration of water with certain characteristics started by reading the temperature of the surrounding air and water in the column.

Then the compressor was switched on and when the first bubbles appear, that is bubbles entered the air distributor the over-pressure value before the distributor $(p_m)_d$ and the orifice plate $(p_m)_p$ was measured, that is the pressure difference in front of and after the orifice plate (Δp_p). Air flow regulation is performed using a flow regulator and relieving valve until a set value for the adopted investigation regime is attained. When the flow is stabilized water sampling from the column in equal time intervals starts ($\Delta\tau = 60$ s) and the dissolved oxygen content is measured until the same value is repeated three times. After one regime is investigated the compressor is switched off and the relieving valve opened completely. Water from the column is released into the drains vie a draining valve. The column is then filled with a fresh amount of water. Thus, the installation is ready for a new investigation regime, that is the described procedure is repeated.

The described device with membrane air distributor for the water phase was used for the measuring of the volume coefficient of the oxygen transport, based on the material balance according to literature [3–5].

3. Determination of technical indicators of examined aeration regimes

The coefficient of oxygen transport in water k_La (obtained as a product k_L and the specific surface of the contact between air and water in the aeration process, a) or oxygen over-pressure relaxation rate constant is a parameter used to determine the transport intensity of oxygen in water, that is the rate the equilibrium state is reached. Experimentally determination by method as prior was described [1,6] according to literature [3–5] is based on the general equation of material balance with complete mixing of oxygen flow through the batch reactor:

$$Q \cdot c_{\mathrm{in}} + \dot{V}_{\mathrm{G}} \cdot c_{\mathrm{ul}} - V_{\mathrm{L}} \cdot R(\tau) = Q \cdot c + \dot{V}_{\mathrm{G}} \cdot c_{\mathrm{iz}} + V_{\mathrm{L}} \cdot \frac{\mathrm{d}c}{\mathrm{d}\tau} \tag{1}$$

The gas phase material balance gives:

$$\dot{V}_{\mathrm{G}} \cdot \left(c_{\mathrm{ul}} - c_{\mathrm{iz}}\right) = A \cdot K_{\mathrm{L}} \cdot \left[c^{*}\left(c_{\mathrm{iz}}\right) - c\right] \tag{1a}$$

The total coefficient of oxygen transport in the water, K_La is dependent from the transport coefficient in the water phase and in air bubbles. If the resistance to transport in air can be neglected, K_L is approxymatelly equal with volume coefficient of oxygen transport in water, k_L:

$$K_{\mathrm{L}}a = k_{\mathrm{L}}a, \quad \mathrm{s}^{-1} \tag{2}$$

It can be determined from the equation:

$$k_{\mathrm{L}}a = \frac{(c_{\mathrm{ul}} - c_{\mathrm{iz}})\,\mathrm{d}V_{\mathrm{G}}}{V_{\mathrm{L}}(c^{*}(c_{\mathrm{iz}}) - c)\,\mathrm{d}\tau}, \quad \mathrm{s}^{-1} \tag{3}$$

$$Qc_{\mathrm{in}} + \frac{\mathrm{d}V_{\mathrm{G}}}{\mathrm{d}\tau}c_{\mathrm{ul}} - V_{\mathrm{L}}R_{\mathrm{O_2}}(\tau) = Qc + \frac{\mathrm{d}V_{\mathrm{G}}}{\mathrm{d}\tau}c_{\mathrm{iz}} + V_{\mathrm{L}}\frac{\mathrm{d}c}{\mathrm{d}\tau} \tag{4}$$

Equilibrium mass concentration of oxygen in water is dependent of oxygen concentration air at the output, based on the Henry law:

$$c^{*}\left(c_{\mathrm{iz}}\right)/\mathrm{c} = c_{\mathrm{iz}}RT/Ha \tag{5}$$

is determined by equation with modified Henry's constant, Hc:

$$Hc = Ha/(R \times T_{\mathrm{G}} \times C_{\mathrm{L}}) \tag{5a}$$

that gives:

$$c^{*}(c_{\mathrm{iz}}) = \frac{c_{\mathrm{iz}}}{Hc} \tag{6}$$

Eqs. (5) and (6) give the expression for calculating the output mass concentration of oxygen in air controlled with the constant outer air pressure in dependence of temperature:

$$c_{\mathrm{iz}} = \frac{Ha(V_{\mathrm{G}}c_{\mathrm{ul}} + Vk_{\mathrm{L}}ac)}{V_{\mathrm{G}}Ha + V_{\mathrm{L}}k_{\mathrm{L}}aRT_{\mathrm{G}}c_{\mathrm{L}}} \tag{7}$$

Time dependence of dissolved oxygen concentration is presented by the following equation:

$$Y = m \cdot X \tag{8}$$

where

$$Y = \ln \frac{\dfrac{p_{\mathrm{ul}}M_{\mathrm{O_2}}}{R\,T_{\mathrm{G}}} - \dfrac{Ha}{R\,T_{\mathrm{R}}c_{\mathrm{L}}}c_{\mathrm{o}}}{\dfrac{p_{\mathrm{ul}}M_{\mathrm{O_2}}}{R\,T_{\mathrm{G}}} - \dfrac{Ha}{R\,T_{\mathrm{R}}c_{\mathrm{L}}}c(\tau)} \tag{9}$$

m = slope coefficient of the equilibrium curve:

$$m = \frac{\dfrac{Ha}{RT_{\mathrm{R}}c_{\mathrm{L}}}k_{\mathrm{L}}a}{\dfrac{Ha}{RT_{\mathrm{R}}c_{\mathrm{L}}} + \dfrac{V_{\mathrm{L}}}{V_{\mathrm{G}}}k_{\mathrm{L}}a} - R_{\mathrm{O_2}}(\tau) \tag{10}$$

$$X = \tau \tag{11}$$

The value of Y is given for each value of $c(\tau)$ determined by experiments for defined time intervals. The previous equations result in the formulae for determining the coefficient of oxygen in wastewater as:

$$k_{\mathrm{L}}a = \frac{Ha(m + R_{\mathrm{O_2}}(\tau))V_{\mathrm{G}}}{V_{\mathrm{G}}Ha - (m + R_{\mathrm{O_2}})V_{\mathrm{L}}RT_{\mathrm{R}}c_{\mathrm{L}}} \tag{12}$$

Based on the known value for the coefficient of oxygen transport (k_La) actual capacity of oxygen (OC) was determined as technical parameters in dependence of examined aeration regimes [6]:

$$(k_{\mathrm{L}}a)_{\mathrm{s}} = \frac{(k_{\mathrm{L}}a)_{t_{\mathrm{L}}}}{\theta^{t_{\mathrm{L}}-20}}, \quad \mathrm{s}^{-1} \tag{13}$$

$$\mathrm{OC} = \left(k_{\mathrm{L}}a\right)_{\mathrm{s}} \cdot c_{\mathrm{s}}^{*} \cdot V_{\mathrm{L}} \tag{14}$$

Standard capacity, OC corresponds to velocity of oxygen dissolution after the total surface between the air and water is achieved. Based on the known value for the coefficient of oxygen transport $(k_L a)_s$ actual capacity of oxygen introduction OC′, as the product of the standard capacity of oxygen introduction and corresponding correction factors that convert standard investigation conditions to real ones are defined [3]:

$$\mathrm{OC}' = \alpha \cdot \mathrm{OC} \cdot \frac{\beta \cdot c_\mathrm{h}^* - c_\mathrm{o}}{c_\mathrm{s}^*} \cdot \theta^{(t_\mathrm{L} - 20)}, \quad \mathrm{kg\ h^{-1}} \tag{15}$$

The actual efficiency of the transport system represents the ratio between the real capacity of oxygen introduction, OC′and G_{O_2}, the total oxygen introduced by the aeration:

$$E' = \frac{\mathrm{OC}'}{G_{\mathrm{O}_2}} = \frac{\mathrm{OC}'}{(V_\mathrm{G})_n \cdot \rho_\mathrm{G} \cdot y_{\mathrm{O}_2}} \cdot 100, \quad \% \tag{16}$$

The values obtained for oxygen pressure relaxation rate constant $(k_L a)_s$ were used to determine the values of real capacity of oxygen introduction,OC′ real oxygen transport efficiency, E'.

Real energy efficiency of oxygen transport E_e is based on the sum of engaged power of all electromotor (for aerator, pump, blower etc. drive).

$$E_\mathrm{e}' = \frac{\mathrm{OC}'}{\sum_i P_i}, \quad \mathrm{kg\ kWh^{-1}} \tag{17}$$

The experimental results (Fig. 2) obtained point out that the technical indicators of the aeration process efficiency for a liquid height of 2 m in the presence of 5 mg l^{-1} of oil in water and air flow of 10 m^3 h^{-1} are significantly improved compared to the ones obtained for flows of 2 and 6 m^3 h^{-1}, while for the same liquid height and oil presence of 10 mg l^{-1} the air flow value does not have a significant influence on technical indicators of the aeration process. For the same concentration of oil in water and the same air flow and water height of 1 m the volume coefficient of oxygen transport is for 25%–40% greater than for aeration with a water height of 2 m and energy efficiency lower [6].

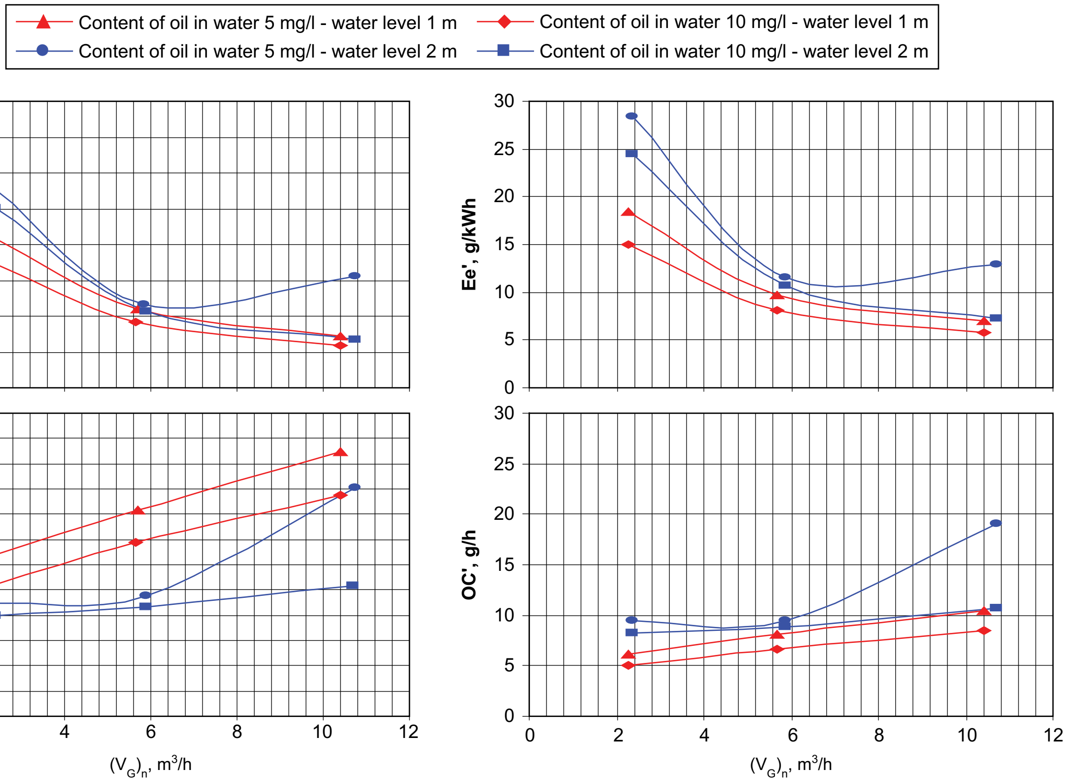

Fig. 2. Technical aeration parameters in dependence of aeration regimes according to Ref. [6] (a) $k_L a_s$, for standard conditions and (b) real capacity of oxygen introduction OC′.

The effects of aeration regimes on experimentally measured volume coefficients of oxygen transport and saturation time were in agreement with theoretically obtained passive rate constant (of diffusion and adsorption process) that controll the solubility degree of oxygen [1].

The intention in present paper is to develope thermodynamic method for diagnostic of electrons concentration in gas bubbles in aerated saturated water in equilibrium with chemisorbed oxygen, as well diagnostic of surface electrons density in PLTE with hydrogen ions enabling stationary surface energy by the change of partially volume of gas bubbles. The best correlation coefficients of determined surface electrons densities with indicators of electrons PLTE could help in understanding the resistances to oxygen transport in gas and liquid phase in dependence of aeration regimes.

4. Determination of electron densities in gas bubbles enabling aeration of refinery wastewater in dependence of aeration regimes

In examined regimes, average liquid temperature of water, 14.1°C was constant inside relative dispersion less than 11% and for examined aeration regimes was defined with Gibbs energy of superoxide anions and dissolution entropy:

$$\Delta G^{\theta}(O_2{}^{-})_{G/L} = 31.84 \text{ kJ mol}^{-1}$$

$$\Delta S^{\theta}(O_2{}^{-})_{G/L} = 110.9 \text{ J mol}^{-1}\text{K}^{-1}$$

$$T_{(l)} = \frac{\Delta G(O_2/O_2{}^{-})_{aq}}{\Delta_{ads}S^{\theta}(O_2)_{G/aq}} = 287.1\text{ K} \tag{18}$$

In examined regimes the monolayer adsorption equilibrium constant to Langmuir, K_{Lg} were determined on the base measured oxygen contents in saturated water and temperature. It was obtained that oxygen transport by monolayer adsorption and desorption is water entropy driven process coupled with hydride generation entropy, ΔS^{θ} (H^{-}) aq = 5.9 J mol^{-1} K^{-1}, for maximal air flow and water height 2 m is determined with liquid water entropy $\Delta S^{\theta}(H_2O)_l$ = 69.9 mol^{-1} K^{-1}:

$$-R \ln K_{Lg}(O_2)_{L/G} = 69.9\text{J mol}^{-1}\text{ K}^{-1} \tag{19}$$

Electrons concentration in monolayer in gas phase in equilibrium with chemisorbed oxygen are determined on the base equilibrium adsorption constant to Langmuir, K_{Lg} and measured difference in equilibrium and stationary oxygen concentration, in dependence of examined aeration regimes, at approximately same water temperature (Table 2):

$$\left[O_2^{-}\right]^{*} \leftrightarrow \left(\left[O_2\right]^{*} - \left[O_2\right]_S\right) + \left[e\right]$$

Table 2

The gas phase temperature, T_G; monolayer volume, $\Delta_r V^{\theta}_{m.l}$ (acc to Eq. (23a)), volume electrons concentrations determined to Langmuir isotherm, $[e]_{ml} = [e]_{ch}$, equal concentration of hydrogen ions in coupled process, $[e]_{couple} = [H^{+},e]_{couple}$

c-h-q	T_G (K)	$[e]_{m.l}$ (mol m^{-3}) Eq. (20)	$\Delta_{couple}V_{(H+,e),}$ (m^3) Eq. (23a)	$[e]_{couple}$ (mol m^{-3}) Eq. (25)
0-2-2	288.5	8.67E5	14.7E-6	1E9
0-2-6	290.6	8.38E5	14.7E-6	1E9
0-2-10	291.7	9.44E5	14.7E-6	0.88E9
5-2-2	286.5	1.1E6	−7.04E-6	1.19E9
5-2-6	287.3	1.1E6	−7.04E-6	1.2E9
5-2-10	286.4	1.27E6	−7.04E-6	1.07E9
10-2-2	289.2	1.3E6	−3.4E-6	1.37E9
10-2-6	290.4	1.25E6	−3.4E-6	1.33E9
10-2-10	288.5	1.53E6	−3.4E-6	1.24E9
5-1-2	287.9	1.63E7	−7.04E-6	1.2E9
5-1-*6*	288.6	1.78E7	−7.04E-6	1.12E9
5-1-10	288.8	1.7E7	−7.04E-6	1.14E9
10-1-2	287.9	1.4E7	−3.4E-6	1.36E9
10-1-6	287.8	1.47E7	−3.4E-6	1.31E9
10-1-10	287.9	1.44 E7	−3.4E-6	1.33E9

$$K_{Lg} = \frac{[\mathrm{e}] \cdot \left([\mathrm{O}_2]^* - [O_2]_{\mathrm{s}}\right)}{[\mathrm{O}_2]^*} \tag{20}$$

$$[\mathrm{e}]_{\mathrm{m.l.}} = K_{\mathrm{Lg}} \frac{([\mathrm{O}_2]^* - [\mathrm{O}_2]_{\mathrm{s}})}{[\mathrm{O}_2]^*} 10^3 \mathrm{mol\ m}^{-3}, \quad K_{\mathrm{L}} \leq 0$$

$$[\mathrm{e}]_{\mathrm{m.l.}} = K_{\mathrm{Lg}} \frac{[\mathrm{O}_2]^*}{([\mathrm{O}_2]* - [\mathrm{O}_2]_{\mathrm{s}})} 10^3 \mathrm{mol\ m}^{-3}, \quad K_{\mathrm{L}} \geq 0 \tag{20a}$$

From electron transfer studies between O_2^- ions generated in alkaline water for dynamic standard potential of the O_2/O_2^- couple, −0.33 V has chosen (on dropping mercury cathode –0.284 V), corresponding to electrons Gibbs energy 31.84 kJ mol^{-1}.

Ionization equilibrium of chemisorbed intermediate state in aerated saturated water after unstable hydroperoxyl as product of ozonide ions decay, polarize contact surface with hydrogen ions ($HO_2 \rightarrow O_2^- + H^+$, p$K$ = 4.8) determine hydrogen positive ions concentration.

Relaxation of surface energy to stationary sum of liquid surface tension and chemical potential of chemisorbed ions, atoms or molecules ($A\sigma + n\mu$ = const), enable surface concentration change ($c^* - c_s$) to Gibbs adsorption isotherm dependent on surface tension change $\Delta\sigma$ in comparison to distilled water:

$$\Gamma = \frac{(c^* - c)}{A} \tag{21}$$

$$\Gamma = \frac{\Delta\sigma}{RT} \tag{22}$$

$$\Delta\sigma A^{\theta} = (c^* - c)RT \tag{22a}$$

Molar or specific contact surface, can to be calculated after stationary surface energy is achieved, based on measured wastewater surface tension difference, $\Delta\sigma$ in comparison with distilled water and temperature:

$$A^{\theta} = \frac{A}{c^* - c}$$

$$\frac{A}{c^* - c} = \frac{RT}{\Delta\sigma} \tag{22b}$$

The monolayer reaction volume $\Delta_r V$ [e, H$^+$], define average monolayer electrons distance from oxygen chemisorbed molecules between the two collisions to Perrine (determined by absolute temperature, water viscosity, η and oxygen diffusion coefficient in ions pair with heavy metals, $D = 10^{-8}$ m^2 s^{-1}):

$$r_{\eta,D} = \frac{k_{\mathrm{B}}T}{6\pi\eta D} \tag{23}$$

$$\Delta_{\mathrm{r}} V_{\mathrm{ml}}{}^{\theta} = \frac{A}{c^* - c} \cdot r_{\eta,D} \tag{23a}$$

According to data in Table 2 in examined regime without added motor increased surface monolayer volume is adsorbed in liquid phase but in the other examined aeration regimes increased volume is adsorbed in gas phase.

Contributed factor of irreversibility of O_2/OH^- pair is faster electron transfer enabling mechanical equilibrium of active volume oxygen transport with passive (diffusion and oxygen adsorption affinity) than the rate of oxygen molecules dissociation. Gas oxygen molecules as a stable intermediate with H ad-atom make possible coupled reaction of electron produced by superoxide oxydation in PLTE and hydrogen ion (Table 2) with equilibrium constant, K_{couple} of coupled process, after PLTE is achieved:

$$\begin{aligned} &\mathrm{O}_2 + \mathrm{e} = \mathrm{O}_2^- && E^{\theta} = -0.33\mathrm{V} \\ &\mathrm{O}_2^- + \mathrm{H}^+ = \mathrm{HO}_2 && \mathrm{E}^{\theta} = -0.12\mathrm{V}\left(\mathrm{p}K = 4.8\right) \end{aligned}$$

$$\begin{aligned} &\mathrm{O}_2 + \mathrm{e} + \mathrm{H}^+ = \mathrm{HO}_2 && \Delta G_{\mathrm{couple}} = \Delta G_1 + \Delta G; \\ & && \Sigma\, \Delta\chi^{\theta} = \pm\, 0.46\mathrm{V} \end{aligned}$$

Calculated equal electrons and hydrogen ions concentrations in coupled process catalyzed by stationary adsorbed superoxide ion can be calculated to Eq. (25):

$$\begin{gathered} [\mathrm{e}]_{\mathrm{couple}} = [\mathrm{e}]_{\mathrm{G}} = \left[\mathrm{H}^+\right]_{\mathrm{G}} \\ K_{\mathrm{couple}} = \frac{([\mathrm{O}_2]^* - [\mathrm{O}_2]_{\mathrm{s}})}{[\mathrm{O}_2]_{\mathrm{s}} [\mathrm{e}] \cdot \left[\mathrm{H}^+\right]} \\ [\mathrm{e}] \cdot \left[\mathrm{H}^+\right] = \frac{\left([\mathrm{O}_2]* - [\mathrm{O}_2]_{\mathrm{s}}\right)}{[\mathrm{O}_2]\, K_{\mathrm{couple}}} \end{gathered} \tag{24}$$

$$\begin{gathered} [\mathrm{e}]_{\mathrm{couple}} = \sqrt{\frac{\left([\mathrm{O}_2]^* - [\mathrm{O}_2]_{\mathrm{s}}\right)}{[O_2]_{\mathrm{s}}\, K_{\mathrm{couple}}}} \\ [\mathrm{e}]_{\mathrm{couple}} = \sqrt{\frac{\left([\mathrm{O}_2]^* - [\mathrm{O}_2]_{\mathrm{s}}\right)}{[\mathrm{O}_2]^*\, 10^{-\frac{0,46}{0,025}}{}_{\mathrm{L}}}} \\ [\mathrm{e}]_{\mathrm{couple}} = 1.58 \times 10^9 \sqrt{\frac{(c* - c_{\mathrm{s}})}{c_{\mathrm{s}_{\mathrm{L}}}}} \end{gathered} \tag{25}$$

Oxygen chemisorbed to Langmuir as superoxide ion is catalyst of coupled process which enable PLTE of electrons distributed by thermal collisions between to energy levels [1]:

- Between chemisorbed electrons (with concentration defined to Eq. (20))
- Hydrogen ions (with concentration defined to Eq. (25)).

Polarization potential is indicator of gas hydrogen ions PLTE, E_{ind} achieved by equal oxygen chemical potential change with electric hydrogen potential change after hydrogen pressure with oxygen over-pressure on air input achieve thermal equilibrium:

$$-\Delta\mu^{\theta}(O_2/OH^-) = F\Delta E(H^+ + e/1/2H_2)_g = FE_{\text{ind}}$$
$$E_{\text{ind}} = \frac{RT_G}{F}\ln\frac{[e]_{\text{couple}}}{\sqrt{\Delta p(H_2)}} \tag{26}$$

The change of surface reaction volume of electrons and hydrogen ions in PLTE with Eq. (27) can be defined:

$$\Delta_r V(H^+, e) = \frac{A \cdot r_{\eta,D}}{c^* - c} \cdot \left[H^+, e\right]_{\text{couple}} \tag{27}$$

PLTE of chemisorbed electrons concentration to Langmuir is achieved by catalytic surface electrons density change, dependent on aeration regime:

$$\Delta[e]_r = \frac{\Delta[e]_{\text{eq}}}{\Delta_{\text{couple}}V(H^+, e)} \tag{28}$$

where is in the end point:

$$\Delta[e]_{\text{ch.}} = \Delta[e]_{\text{m.l.}} = [e]_{\text{eq.}}$$

$$[e]_r = \frac{[e]_{\text{eq}}}{\Delta_{\text{couple}}V(H^+, e)}$$

Surface electrons density, $[e]_r$, mol m^{-6} achieved after transition of chemisorbed electrons in the surface reaction oxygen volume at stationary electric permittivity, ε enable depolarization after equilibrium between hydrated and dehydrated electrons kinetic energy is achieved at depolarization oxygen potential, χ to Eq. (28b):

$$\frac{k_B T(e_{\text{aq}})}{\varepsilon} = \frac{k_B T(e)_{\text{ad}}}{\varepsilon} \tag{28a}$$

Table 3
Absolute temperature of hydrated electrons, T_{eH_2O}, dehydrated electrons T_e, relative electric permittivity of ε_r which enable equilibrium between kinetic energy of hydrated and dehydrated, gas electrons at oxygen depolarization potential, χ

c-h-q	$T_{O_2+e\cdot H_2O}$ (K) Eq. (29)	T_{ePLTE} (K) Eq. (30)	$\varepsilon_r = \frac{T_{e_{aq}}}{T(e)_{ad}}$ Eq. (28a)	χ (V) Eq. (28b)
0-2-2	284.2	87	3.26	0.081
0-2-6	284.2	78	3.515	0.088
0-2-10	284	50	5.68	0.142
	303	503	0.6	0.015
5-2-2	289.5	68.5	4.22	0.105
5-2-6	286.1	41	6.97	0.174
5-2-10	286.1	5.1E4	0.0053	1.32E-4
	339	1E6	0.00034	8E-6
10-2-2	293.6	318	0.92	0.025
10-2-6	293.6	294	1	0.025
10-2-10	291	129	2.2	0.057
	311	798	0.39	0.01
5-1-2	289	79.3	3.64	0.09
5-1-6	289	23.2	12.4	0.311
5-1-10	293.3	191.5	1.53	0.038
10-1-2	294.7	284	1.03	0.026
10-1-6	294.7	116.9	2.52	0.063
10-1-10	294.7	284	1.04	0.026

Table 4
Over pressure measured on air input, $\Delta p_{\text{airin,}}$ energy efficiency of oxygen transport, E_e, hydrogen polarization potential in gas phase E_{ind} and electrons density after transition in the coupled reaction monolayer volume at stationary surface energy $[e]_r$

c-h-q	$\Delta p_{\text{air in.}}$ measured [6]	E'_e g kWh^{-1}, Eq. (17)	$E_{\text{ind}}V$ Eq. (26a)	$[e]_r$ mol m^{-6} Eq. (27)
0-2-2	2.127	35.1	0.41	59
0-2-6	2.392	15.0	0.412	57
0-2-10	3.332	14.8	0.406	73
5-2-2	2.18	28.4	0.412	132
5-2-6	2.473	11.5	0.411	130
5-2-10	0.032	13	0.46	102
10-2-2	2.313	24.5	0.419	278
10-2-6	2.631	10.7	0.417	278
10-2-10	3.215	7.3	0.411	360
5-1-2	1.355	18.4	0.420	1925
5-1-6	1.701	9.8	0.417	2100
5-1-10	2.444	7.06	0.413	2083
10-1-2	1.355	15	0.423	3111
10-1-6	1.674	8.09	0.420	3270
10-1-10	2.444	5.8	0.416	3185

$$\varepsilon_r = \frac{T(\mathrm{e_{aq}})}{T(\mathrm{e})_{\mathrm{ad}}} \quad \text{and} \quad \chi = \varepsilon_r \frac{T_l}{T(\mathrm{e})_{\mathrm{ad}}} \tag{28b}$$

Temperature of electrons enabling oxygen depolarization and partial local equilibrium, PLTE between electrons and heavy particles to be achieved ($T_{\text{ePLTE}} = T(\mathrm{e})_{\mathrm{ad}} = T(\mathrm{e})_{\mathrm{MH_2O}}$) are calculated based on the air pressure on membrane which enable water entropy driven aeration $T(\mathrm{e})_{\mathrm{aq}}$ of depolarized oxygen by electrons hydration (Eq. (29)) and dehydration (Eq. (30):

$$T(\mathrm{e})_{\mathrm{aq}} = \frac{RT_{\mathrm{L}} \ln c\,(\mathrm{O_2}^-)_{\mathrm{L}}}{S^{\theta}\left(\mathrm{H_2O}\right)_{\mathrm{L}}} \tag{29}$$

$$T(\mathrm{e})_{\mathrm{M \cdot H_2O}} = \frac{C_{\mathrm{V,L}}(T(e)_{\mathrm{aq}} - T_{\mathrm{L}})}{R \cdot \ln \dfrac{p_{\mathrm{o}}}{p_{\mathrm{a}}}} \tag{30}$$

Figs. 3 and 4 presents found functionally dependence between surface electrons density change obtained with the best correlation coefficients, $R^2 > 0.7$, by variation of air flow: $q = 2$, 6, and 10 m^3 h^{-1} with the next examined parameters:

- Depolarization surface potential of hydrated electron in liquid phase, χ
- Active polarization potential of dehydrated electrons in PLTE with hydrogen ions, E_{ind}
- Energy efficiency of oxygen transport, E_e

On the base the best found correlation coefficients between examined parameters, for water column height 2 m it can be concluded:

1. In the aeration regimes: 10-2-q, $R^2 = 0.6653$; 10-1-*q*, $R^2 = 0.8677$; and 5-1-*q*, $R^2 = 0.8729$, according to found direct functionally dependence:
   - Energy efficiency of oxygen transport, E_e increase with increased polarization potential of indicator of PLTE, E_{ind}.

   In regime: 5-1-*q*, $R^2 = 0.8999$, energy efficiency of oxygen transport, E_e decrease with increased electrons surface density change.
2. In aeration regimes 0-2-*q*, 5-2-*q* and 10-2-*q*, according to found direct functionally dependence increased electrons density change $[\mathrm{e}]_r$ with air flow:
   - Decrease active polarization of indicator of PLTE ($R^2 = 0.953$, $R^2 = 0.994$, and $R^2 = 0.9423$, respectively)
   - Increase oxygen depolarization surface potential of hydrated surface electron in liquid phase, χ ($R^2 = 0.9524$, $R^2 = 0.7991$ and $R^2 = 1$, respectively), also in aeration regime 10-1-*q*, $R^2 = 0.7837$.
3. In regime without added motor oil, at least electrons density after transition in the monolayer reaction volume in liquid phase maximal energy efficiency was achieved, at the least air flow, by thermal distribution between two energy levels.

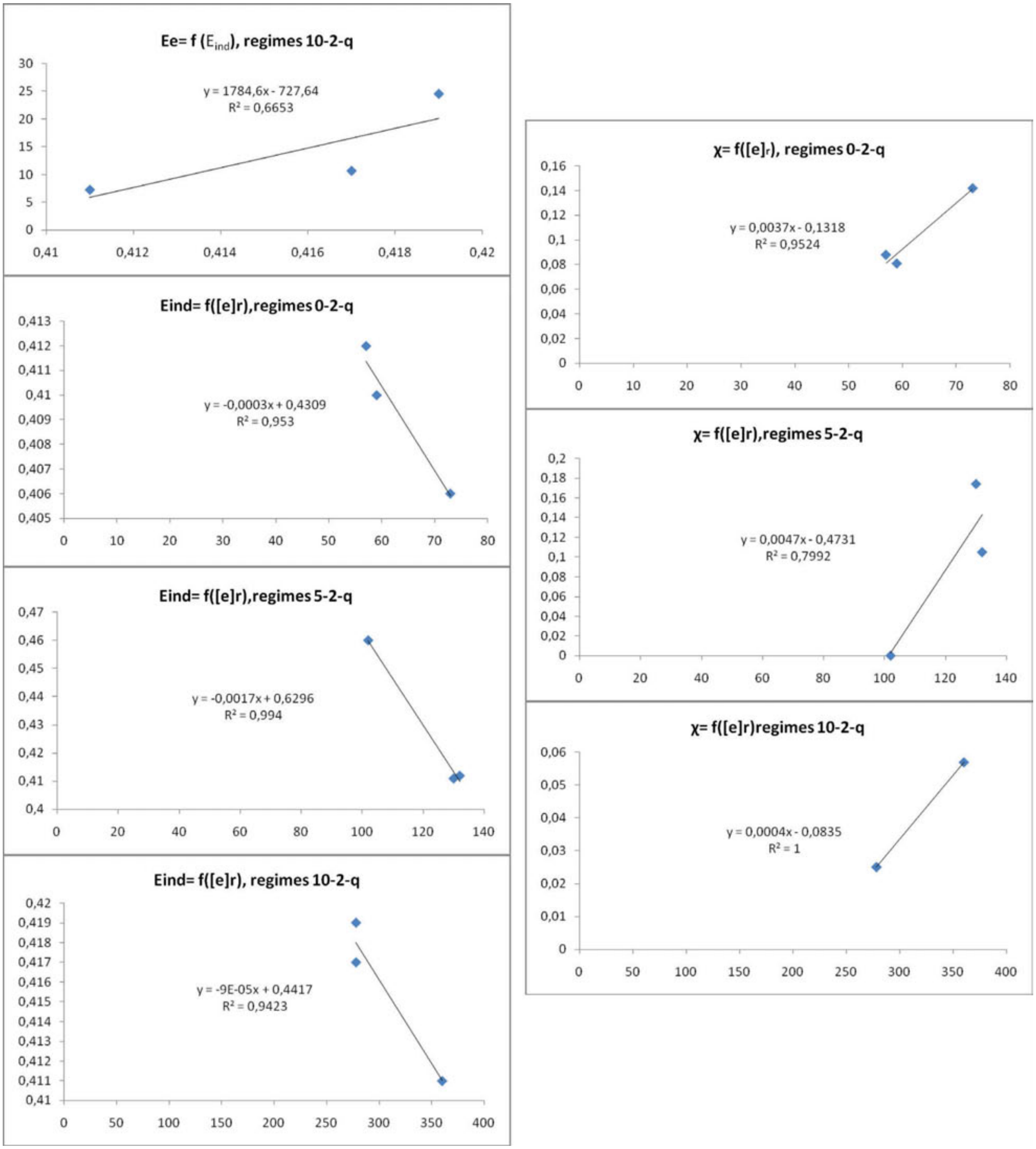

Ee= f (E_{ind}), regimes 10-2-q

Eind= f([e]r),regimes 0-2-q

Eind= f([e]r),regimes 5-2-q

Eind= f([e]r), regimes 10-2-q

χ= f($[e]_r$), regimes 0-2-q

χ= f([e]r),regimes 5-2-q

χ= f([e]r)regimes 10-2-q

Fig. 3. Functional dependence found in aeration regimes with water column height 2 m with the best correlation coefficients between examined parameters.

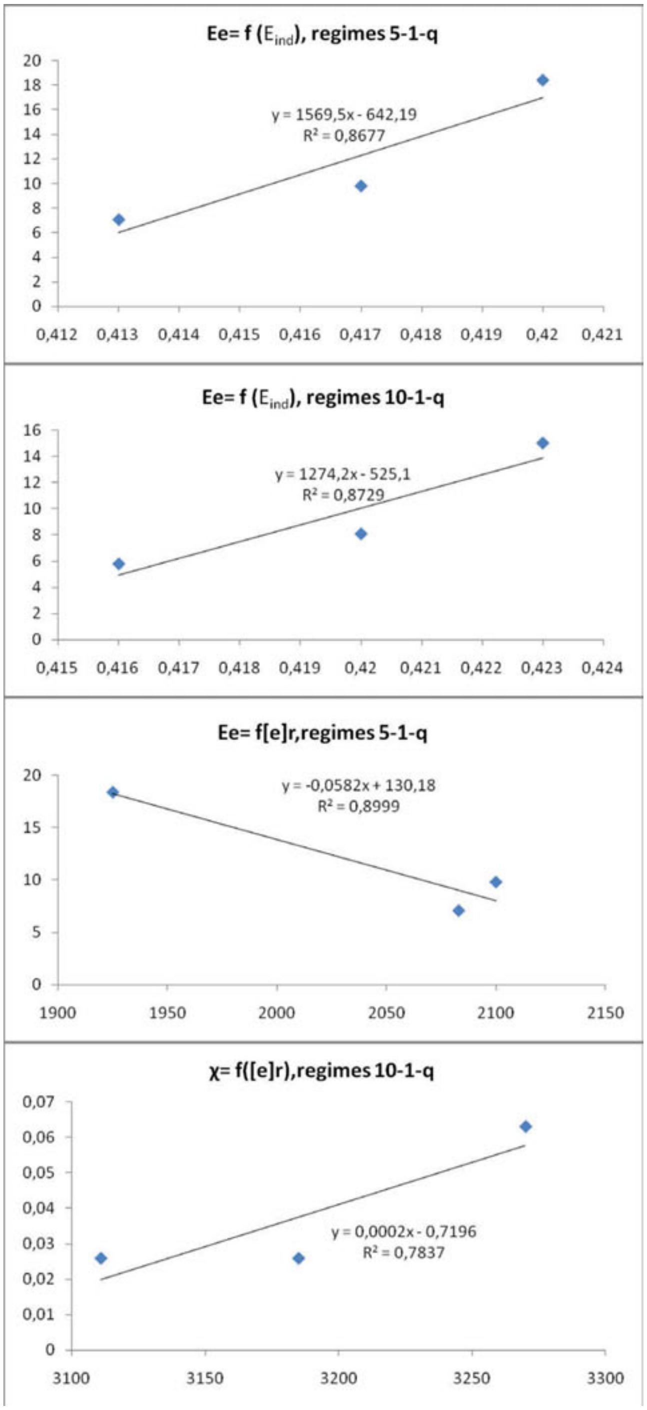

Fig. 4. Functional dependence between examined parameters in aeration regime *s* with water column height 1 m, found with the best correlation coefficient between examined parameters.

5. Conclusions

Method of diagnostic of surface electrons density change in the gas bubbles in aerated saturated refinery wastewater, according to monolayer chemisorptions law and the criteria of partial local thermodynamic equilibrium (PLTE) enable the true understanding of the resistance to oxygen transport in examined aeration regimes, by using the same membrane diffuser.

The experimental results obtained point out that decreased energy efficiency of oxygen transport show functionally dependence with increased surface electrons density change after transition in the monolayer volume with coupled reaction by superoxide ion as catalyst of achieving stationary surface energy:

- Which decreased active oxygen and hydrogen polarization potential in gas bubbles
- Which increased oxygen depolarization potential in monolayer in liquid (or gas) phase

By detailed understanding influence of surface electrons density change in coupled oxygen depolarization and hydrogen polarization the aeration kinetic of thermal or diffusion oxygen mass transport (or the both) could be improved by choosing of optimized aeration regimes.

Symbols

Q — water flow (for batch process conditions $Q = 0$) ($m^3\ s^{-1}$)
c_{in} — mass concentration of oxygen in the influent (kg m^{-3})
$R_{O2}(\tau)$ — specific oxygen consumption during biological treatment (kg $m^{-3}\ s^{-1}$)
c^* — equilibrium mass concentration of oxygen in dependence on the mass concentration of oxygen in air at the output (g m^{-3})
c — mass concentration of oxygen in the influent and effluent (g m^{-3})
c_{ul} — mass concentration of oxygen in air at the input (kg m^{-3})
c_{iz} — mass concentration of oxygen in air at the output (g m^{-3})
a — specific surface of contact between air and water ($m^2\ m^{-3}$)
q or V_G — air flow ($m^3\ s^{-1}$)
V_L — water volume (m^3)
$A = a\ V_L$ — total contact surface between air and water (m^2, kg m^{-3})
a — specific surface of contact between air and water ($m^2\ m^{-3}$)
c_{oil} — added oil content (g m^{-3})
h — water column height (m)
k_La — volume coefficient of oxygen transport (h^{-1})
OC′ — actual capacity (g h^{-1})

E' — technical efficiency (%)

E_e — energy efficiency of oxygen transport (g kWh^{-1})

Ha — Pa·kmol (O_2 + L)/kmol O_2 – Henry's constant in oxygen distribution coefficient between air and water

R — the universal gas constant (J kmol^{-1}·K^{-1})

T_G — absolute air temperature (K)

C_L — molar concentration of water (kmol m^{-3})

$(k_L a)_{fL}$ — oxygen transport coefficient obtained experimentally

t_L — water temperature (°C)

$\theta = 1024$ — temperature correction factor OC, kg h^{-1} standard capacity of oxygen introduction into wastewater

c_s^* — equilibrium mass concentration of dissolved oxygen in clean water, for normal conditions (kg m^{-3})

$\sum_i P_i$ — sum of engaged power of all electromotor (for aerator, pump, blower etc. drive)

$[e]_{m.l}$ — concentration of chemisorbed electrons determined to Langmuir isotherm (mol m^{-3})

$[e]_{couple}$ — concentration of electrons enabling coupled process and PLTE between electrons and hydrogen ions (mol m^{-3})

$\Delta_r V(H^+, e)$ — the change of surface reaction volume of electrons and hydrogen ions in PLTE (m^3)

$\Delta[e]_r$ — surface electrons density change (mol m^{-6})

E_{ind} — hydrogen polarization potential, indicator of PLTE (V)

χ — oxygen depolarization potential (V)

References

[1] M. Ševaljević, M. Stanojević, S. Simić and M. Pavlović, Thermodynamic study of aeration kinetic in treatment of refinery wastewater in bio-aeration tanks, Desalination, 248 (2009) 941–960.

[2] K. Egan-Benck, G. McCarty and W. Winkler Choosing diffusers, Water Environ. Technol., 5(2) (1993) 54–59.

[3] R. Mc Gregor, Diffusion and Sorption in Fibres and Films, Vol. 1, Fiber Chemistry, Marcel Decker, New York, 1973.

[4] J. Montgomery, Water Principles and Design, Wiley, 1985.

[5] John R. Mc Whirter and Joseph. C. hutter, Improved Oxygen Mass Transfer Modeling For Diffused Sibsurface Aeration Systems, Department of Chemical Engineering, The Pennsylvania State University Park, PA 16802, AIChE J., 35(9) (1989) 1527–1534.

[6] N.S. Simic, Influence of System of Aeration on the Efficiency of the Biological Treatment of the Refinery Waste Water, Ph.D. Thesis, Faculty of Mechanical Engineering, Belgrade, Serbia, 2006.